Electron affinity of thallium measured with threshold spectroscopy

C. W. Walter,* N. D. Gibson, and S. E. Spielman
Department of Physics and Astronomy, Denison University, Granville, Ohio 43023, USA

(Received 13 January 2020; revised manuscript received 23 April 2020; accepted 27 April 2020; published 21 May 2020)

The electron affinity of thallium has been precisely measured using laser photodetachment threshold spectroscopy. The relative photodetachment cross section from the negative ion $^{205}Tl^-$ was measured using a tunable infrared laser over the photon energy range 300–900 meV (4130–1380 nm). A pair of closely spaced *s*-wave thresholds were observed due to transitions from the negative ion ground state Tl^- ($6p^2\,^3P_0$) to the two hyperfine levels of the neutral atom ground state Tl ($6p\,^2P_{1/2}$, $F = 0, 1$), which determines the electron affinity of ^{205}Tl to be 320.053(19) meV. These results substantially improve the precision of the Tl electron affinity and resolve long-standing discrepancies in the literature between previous experimental and theoretical values.

DOI: 10.1103/PhysRevA.101.052511

I. INTRODUCTION

Negative ions are of interest for both applied and fundamental reasons [1]. Since the extra electron in a negative ion is not bound by a net Coulomb field, electron correlations are crucial in negative ions. The binding energy of a negative ion (corresponding to the electron affinity of the neutral) is extremely sensitive to multielectron interactions; thus, negative ions serve as important tests of detailed atomic structure calculations and yield key insights into dynamical correlation effects.

Three experimental techniques have emerged as the primary methods for high-precision measurement of atomic electron affinities: tunable laser photodetachment threshold spectroscopy (which is used in the present study) [2,3]; slow electron velocity map imaging (SEVI) [4–6]; and the exquisitely sensitive photodetachment microscope method [7–10]. The electron affinities (EAs) of most elements have now been well established with measured precisions of $<\sim$0.1 meV and agreement between theory and experiment at the few meV level [10–12]. However, the EAs of the group 13 elements (B, Al, Ga, In, and Tl) have been particularly challenging to pin down in part because their negative ions are weakly bound [10–12]; for example, the EA of gallium (Ga) was only very recently definitively established by our group [13]. Prior to the present study, the EA of thallium (Tl) remained as one of the least well determined of all elements outside of the lanthanides and actinides, with differences of $\sim$60 meV or more between previous experimental and theoretical values [10]. The present study resolves the discrepancy for the EA of Tl through high-precision measurement of the binding energy of its negative ion Tl^-.

The ground-state valence configuration of neutral Tl ($Z = 81$) is $6p\,^2P_{1/2}$. Tl has two stable isotopes, mass 203 (30% natural abundance) and mass 205 (70%); only the more abundant heavier isotope was studied in the present experiments. The nuclear spin of ^{205}Tl is $I = 1/2$, resulting in the ground state being split into two hyperfine levels ($F = 0, 1$) separated by 21.310 835(5) GHz (0.088 134 53(2) meV) [14], with $F = 0$ being the lowest energy level. The first fine-structure excited level of Tl ($^2P_{3/2}$) is at an energy of 966 meV [15], which is beyond the present photon energy range.

The configuration of the ground state of the negative ion Tl^- is $6p^2\,^3P_0$, and it has no hyperfine splitting because $J = 0$. An experimental investigation of Tl^- was performed by Carpenter *et al.* [16] using fixed-frequency laser photodetachment electron spectroscopy yielding 377(13) meV for the EA of Tl. The photodetachment signal in that study did not show any contributions from excited fine-structure levels of the negative ion. A large number of theoretical studies of the EA of Tl have been reported using a variety of calculational methods [10,17–23]. There is little agreement in the calculated EAs, with most values ranging from 270 to 400 meV (see Table I for a summary of theoretical results). A very recent calculation by Finney and Peterson yielded an EA of 320(22) meV [10], which is substantially lower than the experimental value of 377(13) meV of Carpenter *et al.* [16] and well outside of the combined uncertainty ranges. Clearly, further study is needed due to the substantial discrepancies between previous theoretical and experimental values.

In the present study, photodetachment threshold spectroscopy with a tunable midinfrared laser was used to precisely measure the binding energy of the $^{205}Tl^-$ ($6p^2\,^3P_0$) ground state to be 320.053(19) meV. No evidence of excited states of Tl^- was observed, indicating that the fine-structure excited levels are either not bound or too weakly bound to be detected in the present experiment. The present results substantially improve the precision of the Tl electron affinity, yielding a value in excellent agreement with the very recent theoretical calculations of Finney and Peterson [10], thus resolving the long-standing previous discrepancies. These results complete the high-precision measurement of the electron affinities of group 13 elements (B, Al, Ga, In, and Tl), facilitating useful comparisons in this column of the periodic table.

*walter@denison.edu

TABLE I. Comparison of the present results for the electron affinity of Tl to previous measurements and theoretical calculations. Methods - Experiment: LPTS = laser photodetachment threshold spectroscopy, LPES = laser photodetachment electron spectroscopy; Theory: CIPSI = multireference configuration interaction, MCDF = multiconfiguration Dirac-Fock, RCC = relativistic Fock-space coupled cluster, HF-DFT = Hartree-Fock density-functional theory, IHFSCC = intermediate Hamiltonian Fock-space coupled cluster, MCDHF = multiconfiguration Dirac-Hartree-Fock, RCC-FPD = relativistic coupled-cluster version of the Feller-Peterson-Dixon composite method.

Study	Method	Electron affinity (meV)
Experiment		
Present	LPTS	320.053(19)
Carpenter *et al.* [16]	LPES	377(13)
Theory		
Arnau *et al.* [17]	CIPSI	270
Wijesundera [18]	MCDF	291
Eliav *et al.* [19]	RCC	400(50)
Chen and Ong [20]	HF-DFT	388
Figgen *et al.* [21]	IHFSCC	347
Li *et al.* [22]	MCDHF	290(15)
Felfli *et al.* [23]	Regge pole	2415
Finney and Peterson [10]	RCC-FPD	320(22)

II. EXPERIMENTAL METHOD AND MEASURED SPECTRUM

In the present experiments, photodetachment from Tl^- was measured as a function of photon energy using a crossed ion-beam—laser-beam system that has been described in detail previously [24,25]. Negative ions were produced by a cesium sputter ion source (NEC SNICS II) [26] using a cathode packed with solid Tl pellets. The ions were accelerated to 12 keV and the $^{205}Tl^-$ isotope was magnetically mass selected; typical currents of Tl^- were only ∼15 pA. In the interaction region, the ion beam was intersected perpendicularly by a pulsed laser beam. Following the interaction region, residual negative ions were electrostatically deflected into a Faraday cup, while neutral atoms produced by photodetachment continued undeflected to a multidynode particle multiplier detector. The neutral atom signal was normalized to the ion-beam current and the laser photon flux measured for each laser pulse. The spectra were obtained by continuously scanning the laser wavelength over a range repeatedly and then sorting the data into photon energy bins of selectable width, as previously described by Walter *et al.* [24].

The laser system consisted of a tunable optical parametric oscillator-amplifier (OPO-OPA) (LaserVision) pumped by a pulsed Nd:yttrium aluminum garnet laser. Both the "signal" and "idler" output bands of the OPA were used in the present measurements, giving an operating range of 250–920 meV (5000–1350 nm). Broad scans across the tuning range were performed with the pump laser operating broadband giving an OPA bandwidth of ∼0.1 meV, while narrow scans near threshold were performed with injection seeding of the pump laser to reduce the OPA bandwidth to ∼0.01 meV. The wavelength

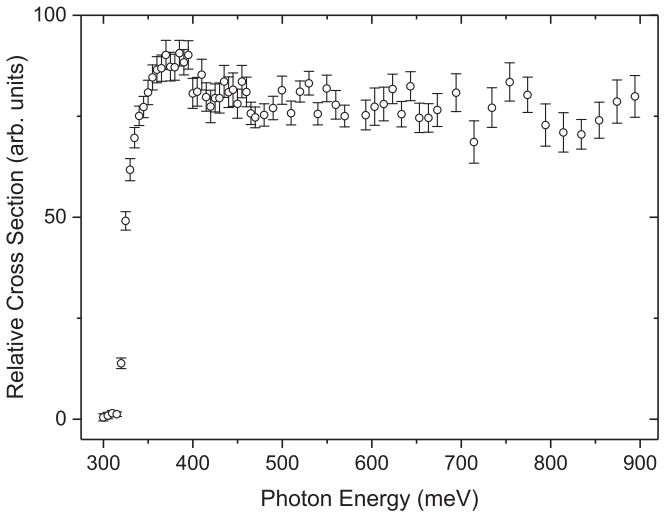

FIG. 1. Measured photodetachment spectrum from Tl^- showing data points (circles) that include 1σ statistical error bars. A single threshold is observed near 320 meV with no significant signal at lower energies, indicating that Tl^- has only one bound state.

of the midinfrared light was determined for each laser pulse using a procedure fully described in Ref. [24]; briefly, a pulsed wave meter (High Finesse WS6–600) measured the wavelength of the OPO signal light, which was then used with the measured pump laser wavelength to determine the wavelength of the OPA light by conservation of energy. The laser beam diverges slightly as it leaves the OPA, so a long focal length lens (∼2-m focal length) was placed in the beam path ∼2 m from the interaction region to approximately collimate the beam. In the interaction region, the laser pulse had a typical energy of ∼50 μJ, pulse duration of ∼5 ns, and beamwidth of ∼0.25 cm. To reduce room air absorption by strong H_2O and CO_2 bands in the midinfrared [27], a tube flushed with dry nitrogen gas was used to enclose the laser-beam path from the OPA to the vacuum chamber entrance window.

The relative photodetachment cross section from Tl^- measured over the photon energy range 300–900 meV is shown in Fig. 1. This spectrum shows a single photodetachment threshold near 320 meV. There is no observable photodetachment signal below the threshold, indicating that there is no significant population of more weakly bound excited states in the negative ion beam. Since no threshold structure was observed at higher photon energies, the threshold near 320 meV is identified as due to the opening of photodetachment from the ground state of Tl^- ($6p^2\,{}^3P_0$) to the neutral atom ground state Tl ($6p\,{}^2P_{1/2}$).

For a limited range above an opening threshold, the photodetachment cross section is characterized by the Wigner threshold law [28]:

$$\sigma = \sigma_0 + a(E - E_t)^{\ell+(1/2)}, \tag{1}$$

where E is the photon energy, E_t is the threshold energy, ℓ is the orbital angular momentum of the departing electron, and a is a scaling constant. The background cross section due to photodetachment to lower energy thresholds is represented by σ_0. In the present experiments, a p electron is detached from the Tl^- ion; thus, the angular momentum selection rule

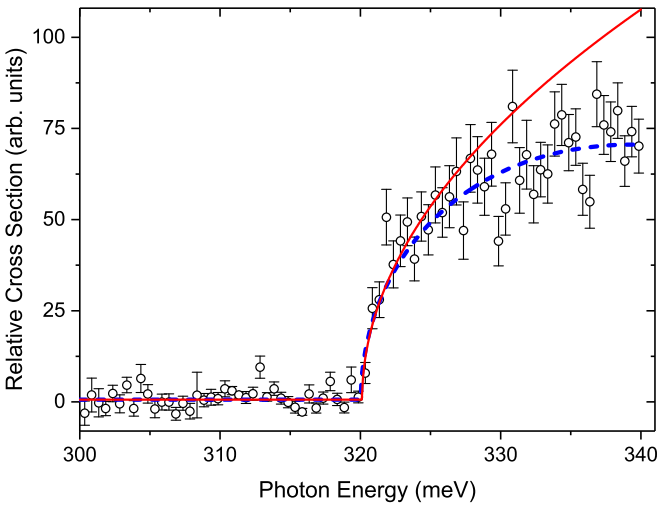

FIG. 2. Measured photodetachment spectrum from Tl^- (circles) showing the single threshold observed in the present study with fits to theoretical functional forms. The pure s-wave Wigner law [Eq. (1) with $\ell = 0$] (red solid line) fit over the first 5 meV above threshold deviates significantly from the data at higher photon energies. The s-wave Wigner law with leading correction function [Eq. (2)] (blue dashed line) fit over the entire range follows the data much better.

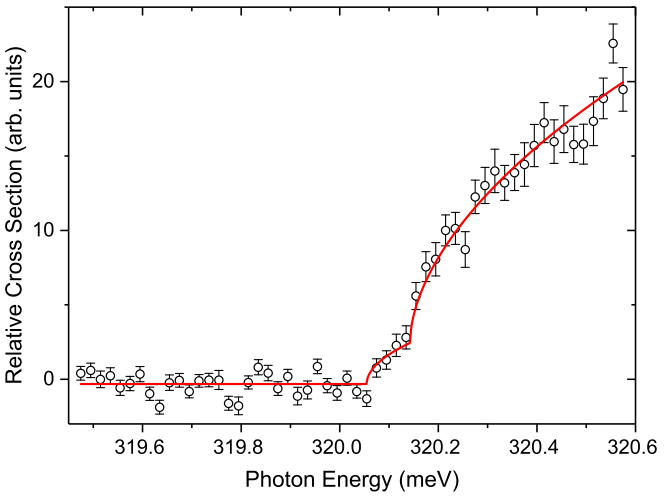

FIG. 3. Narrow scan near the threshold for the Tl^- ($^3P_0$) to Tl ($^2P_{1/2}$) ground-state to ground-state transition using the seeded laser; the bin width of 0.02 meV chosen for processing the measured data (circles) in this figure is approximately twice the bandwidth of the laser (∼0.01 meV). The solid line is a fit of the pure s-wave Wigner law [Eq. (1)] with two nested detachment thresholds to the $F = 0$ and 1 levels of Tl ($^2P_{1/2}$) separated by the hyperfine splitting of 0.088 134 53(2) meV [14]. The lower-energy threshold corresponds to the electron affinity of ^{205}Tl.

$\Delta\ell = \pm 1$ dictates that the departing electron will be either s or d; near threshold, the s wave ($\ell = 0$) dominates the cross section.

As the energy above threshold increases, the photodetachment cross section progressively deviates from the Wigner law due to long-range interactions between the departing electron and the remaining neutral atom, such as polarization forces [29]. Farley [30] derived an expression for the leading term correction to the Wigner law based on the zero core contribution model of photodetachment [31], which for detachment of a p electron gives the following modified s-wave Wigner law with leading correction:

$$\sigma = \sigma_0 + a(E - E_t)^{1/2} + b(E - E_t)^{3/2}. \qquad (2)$$

The additional term depending on energy above threshold to the 3/2 power has a negative scaling coefficient b, leading to progressively larger reductions in the cross section relative to the pure s-wave Wigner law as the energy increases.

Figure 2 shows the photodetachment spectrum in the vicinity of the threshold with fits of the theoretical functions. The pure s-wave Wigner law [Eq. (1) with $\ell = 0$] fit over the first 5 meV above threshold deviates significantly from the data at higher photon energies. The s-wave Wigner law with leading correction function [Eq. (2)] fit over the entire range follows the data much better. While deviation from the pure s-wave Wigner law occurs as little as a few meV above the threshold, the s wave with leading correction function provides a reasonable representation of the data up to at least 20 meV above threshold. At higher energies above the threshold region, other effects become important, and the threshold functions are no longer applicable.

In order to precisely determine the threshold energy and thus the electron affinity, narrow scans were taken near the thresholds with the pump laser seeded to reduce the bandwidth to ∼0.01 meV. A high-resolution scan near threshold is shown in Fig. 3. The spectrum shows two closely spaced s-wave thresholds due to photodetachment from the negative ion ground state Tl^- ($6p^2\,^3P_0$) to the two hyperfine levels of the neutral atom ground state Tl ($6p\,^2P_{1/2}$, $F = 0, 1$). A fit of the pure s-wave Wigner law [Eq. (1)] with two nested thresholds separated by the hyperfine splitting of ^{205}Tl ($^2P_{1/2}$) of 0.088 134 53(2) meV [14] gives an excellent representation of the data in the narrow range of Fig. 3. Over the range of only 0.5 meV above threshold, no significant deviation from the pure s-wave Wigner law was observed, so the higher-order terms in the cross-section function were found to be insignificant this close to threshold. Furthermore, note that the small separation of the two hyperfine thresholds is insignificant over the larger photon energy ranges of the photodetachment spectrum shown in Figs. 1 and 2.

The weaker lower-energy threshold in Fig. 3 is due to detachment to $F = 0$, while the stronger higher-energy threshold is due to detachment to $F = 1$. The relative strengths of the two hyperfine channels can be estimated based on general theoretical considerations, as discussed, for example, in Blondel *et al.* [9] or Bilodeau and Haugen [32]. For the present case of detachment from $^3P_0$ to $^2P_{1/2}$ with nuclear spin $I = 1/2$, the predicted relative strength reduces to simply $(2F + 1)$; thus the $F = 1$ channel is predicted to be 3 times stronger than $F = 0$. The average fitted relative strength of the two channels for the near-threshold data is 2.4(10), matching the expected ratio although the uncertainty in this value is substantial. Fits were also performed with both the energy separation between the two thresholds and the ratios of strengths allowed to vary; the fitted separation was found to be 0.07(3) meV, which agrees well with the accepted $F = 0$ to 1 splitting of 0.088 134 53(2) meV [14].

The threshold energy measured in the present experiments for detachment from $^{205}Tl^-$ ($6p^2\,^3P_0$) to the lower-energy $F = 0$ level of Tl ($^2P_{1/2}$) is 320.053(19) meV, which corresponds to the electron affinity of ^{205}Tl. The final result for the threshold energy was obtained by weighted average of fits of the narrow-bandwidth data performed with the spacing between the two thresholds held fixed at the known hyperfine splitting of neutral Tl [14] and the relative hyperfine channel strengths allowed to vary. Fits were also performed of this near-threshold data with bin widths ranging from 0.005 to 0.02 meV (i.e., from half to twice the laser bandwidth) and the fitted threshold energies were found to agree within uncertainties. The quoted 1σ uncertainty in the electron affinity includes statistical uncertainties associated with the fits, photon energy calibration and bandwidth uncertainties, and potential Doppler shifts due to possible deviation of the ion and laser-beam intersection angle from perpendicular (estimated to be within $\pm 5°$ of perpendicular, which gives a Doppler shift uncertainty of 0.010 meV). Also note that in the present experiment, any possible shift of the threshold due to the ponderomotive effect [33] is negligible because the laser beam is not focused so the peak intensity of the laser pulse is relatively low ($\sim 5 \times 10^4\,\mathrm{W/cm^2}$) giving a shift of only $\sim 1 \times 10^{-4}$ meV [13].

III. RESULTS AND DISCUSSION

The measured electron affinity of ^{205}Tl determined in the present study is 320.053(19) meV. For comparison, previous experimental and theoretical values are listed in Table I. The present measured EA is significantly different from the previous measurement of 377(13) meV by Carpenter *et al.* [16]. Carpenter *et al.* used the technique of laser photodetachment electron spectroscopy (LPES), in which the kinetic energies of the ejected electrons were measured following photodetachment with a fixed-frequency laser. This technique is very good for obtaining exploratory information about a negative ion; however, the precision is limited and the calibration of the absolute kinetic energy scale for the photoelectrons is a substantial challenge [1,11,12]. In contrast, the laser photodetachment threshold spectroscopy technique used in the present study relies on the straightforward measurement of laser wavelengths to calibrate the energy scale. The high-precision threshold measurement in the present study significantly shifts the EA of Tl lower than the previous LPES value by 57 meV [16], which is substantially larger than the uncertainty of the previous value (13 meV), indicating that there may have been some calibration errors in that measurement. The present measurement also reduces the uncertainty of the EA by a factor of more than 600 from 13 to 0.019 meV.

As shown in Table I, most of the previous theoretical calculations of the EA of Tl differ from the present measurement by ~30–80 meV. However, the very recent calculation by Finney and Peterson of 320(22) meV [10] is in excellent agreement with the present value of 320.053(19) meV. The calculated electron affinity by Felfli *et al.* of 2415 meV using the Regge pole method [23] is much larger than the present measurement. However, it should be noted that Felfli *et al.*'s calculations also predict two excited states of Tl^- with binding energies of 281 and 66.4 meV; the calculated binding energy of this first excited state is reasonably close to the present measured Tl^- binding energy. While our experiment cannot rule out the existence of a more strongly bound ground state of Tl^- as predicted by Felfli *et al.* [23], several pieces of evidence support the assignment of the present photodetachment threshold value of 320.053(19) meV as the electron affinity of ^{205}Tl. The present measurement is consistent in magnitude with other theoretical calculations, especially that of the recent calculation by Finney and Peterson [10] which is within 1 meV of the present value. Furthermore, Finney and Peterson noted that their calculations showed no indications that the ground state of Tl is not ($^3P_0$), giving further confidence in our assignment of the observed threshold.

In the present experiment, there is no observable photodetachment signal at lower photon energies below the Tl^- ($^3P_0$) ground-state threshold, which indicates that the fine-structure excited states of Tl^- ($^3P_1$ and $^3P_2$) are likely not bound. This inference is consistent with Hotop and Lineberger's estimated Tl^- fine-structure separations of 430(50) meV for $J = 0$–1 and 630(50) meV for $J = 0$–2 based on isoelectronic extrapolation [34]. Because these estimated separations are significantly greater than the present measured binding energy of the $^3P_0$ ground state of 320.053(19) meV, it is reasonable to conclude that the fine-structure excited states are probably not bound; this was also suggested by Hotop and Lineberger [34]. It is also worthwhile to note that the large fine-structure splittings of Tl^- are not surprising, given the large fine-structure splittings of the neutral atom ground states of both Tl ($^2P_{1/2} - {}^2P_{3/2}$) and Pb ($^3P_0 - {}^3P_1$) (isoelectronic to Tl^-), which are 966 and 969 meV, respectively [15].

It is worthwhile to consider the expected magnitude of the isotope shift between the electron affinity of ^{205}Tl measured in the present study and that of the other stable isotope of thallium, ^{203}Tl. Given the weakness of the Tl^- ion beam in the present experiments, it was not possible to carry out measurements on the less abundant mass-203 isotope. However, insights can be gained by comparison to published results for isotopes shifts in negative ions of the next-heavier element, lead. Chen and Ning used the SEVI method to measure the binding energies of Pb^- ($6p^3\,^4S_{3/2}$) relative to the Pb ($6p^2\,^3P_2$) excited state for isotopes 206, 207, and 208 [5]. Their results gave a difference between the binding energies of mass-206 and mass-208 of $-0.40(18)\,\mathrm{cm^{-1}}$ [−0.050(22) meV]. Subsequently, Bresteau *et al.* used the photodetachment microscope method to measure the isotope-averaged electron affinity of Pb^- [35]. As part of that study, they thoroughly evaluated available information on isotope shifts measured for neutral atom bound–bound transitions in Pb and Bi (isoelectronic to Pb^-), which yielded an estimate for the shift of the EA across naturally occurring Pb isotopes (masses 206, 207, 208) of probably not larger than $0.02\,\mathrm{cm^{-1}}$ (0.0025 meV). The results of these two studies are substantially different for the magnitude of the isotope shift in the binding energy of Pb^-, with the former being on the order of the present precision and the latter indicating a much smaller estimated shift. Therefore, given this unsettled situation, we quote our measured EA for thallium as referring to the mass-205 isotope, reserving

TABLE II. Recommended electron affinities for group 13 elements.

Element	Electron affinity (meV)
Boron [36]	279.723(25)
Aluminum [37]	432.83(5)
Gallium [6]	301.166(14)
Indium [24]	383.92(6)
Thallium [present]	320.053(19)

judgment on whether the mass-203 isotope would have a significantly different EA at the present level of precision.

The present measurement of the electron affinity of Tl completes the high-precision measurement of EAs for all of the group 13 elements (see Table II). Comparison shows that there is not a regular trend in the strength of the EA moving down the column, as the values bounce around by more than 100 meV. In comparing the values, one must keep in mind that the heavier elements, especially Tl, have very large fine-structure splittings, which may be different between the neutral atom and negative ion. Nevertheless, the observed variation indicates the significant effects of core-valence interactions and highlights the important role of electron correlations for the binding energies of negative ions. The high-precision data now available for the complete column provide a useful opportunity for detailed systematic theoretical investigations.

IV. SUMMARY

In summary, we have used photodetachment threshold spectroscopy to determine the electron affinity of ^{205}Tl to be 320.053(19) meV. The present result significantly revises the experimental value of the EA of Tl, reduces its uncertainty by a factor of more than 600, and resolves discrepancies between previous experiment and theory. The precise information now available for the negative ion of thallium can serve as a test for evaluating theoretical approaches to atomic structure calculations involving multielectron interactions and correlation effects in heavy elements.

The present results can be extended to further studies of heavy negative ions using threshold spectroscopy. One possible future measurement could be the isotope shift of the EA between ^{205}Tl and ^{203}Tl. A similar experiment could be done to measure the shifts in the EA of isotopes of Pb, which might be able to resolve the discrepancies in previous studies [5,35].

ACKNOWLEDGMENTS

We thank D. Burdick, K. Patel, R. Drumm, Y. Li, and S. Miller for technical assistance. This material is based in part upon work supported by the National Science Foundation under Grants No. 1404109 and No. 1707743. S.E.S. received partial support from the Laurie Bukovac Hodgson and David Hodgson Endowed Fund at Denison University.

[1] D. J. Pegg, Rep. Prog. Phys. **67**, 857 (2004).
[2] D. M. Neumark, K. R. Lykke, T. Andersen, and W. C. Lineberger, Phys. Rev. A **32**, 1890 (1985).
[3] P. Andersson, A. O. Lindahl, C. Alfredsson, L. Rogstrom, C. Diehl, D. J. Pegg, and D. Hanstorp, J. Phys. B: At. Mol. Opt. Phys. **40**, 4097 (2007).
[4] Z. Luo, X. Chen, J. Li, and C. Ning, Phys. Rev. A **93**, 020501(R) (2016).
[5] X. Chen and C. Ning, J. Chem. Phys. **145**, 084303 (2016).
[6] R. Tang, X. Fu, Y. Lu, and C. Ning, J. Chem. Phys. **152**, 114303 (2020).
[7] C. Blondel, C. Delsart, and F. Dulieu, Phys. Rev. Lett. **77**, 3755 (1996).
[8] C. Valli, C. Blondel, and C. Delsart, Phys. Rev. A **59**, 3809 (1999).
[9] C. Blondel, C. Delsart, C. Valli, S. Yiou, M. R. Godefroid, and S. Van Eck, Phys. Rev. A **64**, 052504 (2001).
[10] B. A. Finney and K. A. Peterson, J. Chem. Phys. **151**, 024303 (2019); **151**, 159901(E) (2019).
[11] T. Andersen, H. K. Haugen, and H. Hotop, J. Phys. Chem. Ref. Data **28**, 1511 (1999).
[12] T. Andersen, Phys. Rep. **394**, 157 (2004).
[13] N. D. Gibson, C. W. Walter, C. Crocker, J. Wang, W. Nakayama, J. N. Yukich, E. Eliav, and U. Kaldor, Phys. Rev. A **100**, 052512 (2019).
[14] A. Lurio and A. G. Prodell, Phys. Rev. **101**, 79 (1956).
[15] A. Kramida, Yu. Ralchenko, J. Reader, and NIST ASD Team, *NIST Atomic Spectra Database* (version 5.6.1), National Institute of Standards and Technology, Gaithersburg, MD (2018), available at https://physics.nist.gov/asd.
[16] D. L. Carpenter, A. M. Covington, and J. S. Thompson, Phys. Rev. A **61**, 042501 (2000).
[17] F. Arnau, F. Mota, and J. J. Novoa, Chem. Phys. **166**, 77 (1992).
[18] W. P. Wijesundera, Phys. Rev. A **55**, 1785 (1997).
[19] E. Eliav, Y. Ishikawa, P. Pyykkö, and U. Kaldor, Phys. Rev. A **56**, 4532 (1997).
[20] G.-X. Chen and P. P. Ong, J. Phys. B: At. Mol. Opt. Phys. **32**, 5351 (1999).
[21] D. Figgen, A. Wedig, H. Stoll, M. Dolg, E. Eliav, and U. Kaldor, J. Chem. Phys. **128**, 024106 (2008).
[22] J. Li, Z. Zhao, M. Andersson, X. Zhang, and C. Chen, J. Phys. B: At. Mol. Opt. Phys. **45**, 165004 (2012).
[23] Z. Felfli, A. Z. Msezane, and D. Sokolovski, J. Phys. B : At. Mol. Opt. Phys. **45**, 189501 (2012).
[24] C. W. Walter, N. D. Gibson, D. J. Carman, Y.-G. Li, and D. J. Matyas, Phys. Rev. A **82**, 032507 (2010).
[25] C. W. Walter, N. D. Gibson, Y.-G. Li, D. J. Matyas, R. M. Alton, S. E. Lou, R. L. Field, III, D. Hanstorp, L. Pan, and D. R. Beck, Phys. Rev. A **84**, 032514 (2011).
[26] R. Middleton, *A Negative-Ion Cookbook* (University of Pennsylvania, Philadelphia, PA, 1990).
[27] L. S. Rothman, I. E. Gordon, A. Barbe *et al.*, J. Quant. Spectrosc. Radiat. Transfer **110**, 533 (2009).

[28] E. P. Wigner, Phys. Rev. **73**, 1002 (1948).
[29] T. F. O'Malley, Phys. Rev. **137**, A1668 (1965).
[30] J. W. Farley, Phys. Rev. A **40**, 6286 (1989).
[31] R. M. Stehman and S. B. Woo, Phys. Rev. A **20**, 281 (1979).
[32] R. C. Bilodeau and H. K. Haugen, Phys. Rev. A **64**, 024501 (2001).
[33] M. D. Davidson, J. Wals, H. G. Muller, and H. B. van Linden van den Heuvell, Phys. Rev. Lett. **71**, 2192 (1993).
[34] H. Hotop and W. C. Lineberger, J. Phys. Chem. Ref. Data **4**, 539 (1975).
[35] D. Bresteau, C. Drag, and C. Blondel, J. Phys. B: At. Mol. Opt. Phys. **52**, 065001 (2019).
[36] M. Scheer, R. C. Bilodeau, and H. K. Haugen, Phys. Rev. Lett. **80**, 2562 (1998).
[37] M. Scheer, R. C. Bilodeau, J. Thogersen, and H. K. Haugen, Phys. Rev. A **57**, R1493 (1998).